

CSF 14–3-3 zeta(ζ) isoform is associated with tau pathology and cognitive decline in Alzheimer's disease

Qiang Qiang^{a,b}, Loren Skudder-Hill^{c,d}, Tomoko Toyota^b, Zhe Huang^b, Wenshi Wei^a, Hiroaki Adachi^{b,*}, Alzheimer's Disease Neuroimaging Initiative¹

^a Department of Neurology, Cognitive Disorders Center, Huadong Hospital, Fudan University, Shanghai, China

^b Department of Neurology, University of Occupational and Environmental Health School of Medicine, Kitakyushu, Japan

^c Yuquan Hospital, Tsinghua University School of Clinical Medicine, Beijing, China

^d School of Medicine, University of Auckland, Auckland, New Zealand

ARTICLE INFO

Keywords:

Alzheimer's disease
14–3-3 zeta(ζ)
Tau pathology
CSF
Dementia

ABSTRACT

14–3-3 is a family of conserved proteins that consist of seven isoforms which are highly expressed in the brain, and 14–3-3 zeta(ζ) is one of the isoforms encoded by the YWHAZ gene. Previous studies demonstrated that 14–3-3 ζ is deposited in the neurofibrillary tangles of Alzheimer's disease (AD) brains, and that 14–3-3 ζ interacts with tau from the purified neurofibrillary tangles of AD brain extract. The present study examined the cerebrospinal fluid (CSF) 14–3-3 ζ levels of 719 participants from the Alzheimer's Disease Neuroimaging Initiative (ADNI), including cognitively normal (CN) participants, patients with mild cognitive impairment (MCI) and patients with AD dementia, and aimed to identify whether CSF 14–3-3 ζ is associated with tau pathology. CSF 14–3-3 ζ levels were increased in AD, and particularly elevated among tau pathology positive individuals. CSF 14–3-3 ζ levels were associated with CSF phosphorylated tau 181 (p-tau) ($r = 0.741$, $P < 0.001$) and plasma p-tau ($r = 0.293$, $P < 0.001$), which are fluid biomarkers of tau pathology, and could predict tau pathology positive status with high accuracy (area under the receiver operating characteristic curve [AUC], 0.891). CSF 14–3-3 ζ levels were also correlated to synaptic biomarker CSF GAP-43 ($r = 0.609$, $P < 0.001$) and neuroinflammatory biomarker CSF sTREM-2 ($r = 0.507$, $P < 0.001$). High CSF 14–3-3 ζ levels at baseline were associated with progressive decline of cognitive function and neuroimaging findings during follow up. In conclusion, this study suggests that CSF 14–3-3 ζ is a potential biomarker of AD that may be useful in clinical practice.

1. Introduction

Alzheimer's disease (AD) is the most common form of neurodegenerative dementia worldwide. The characteristic neuropathological features of AD include the extracellular aggregation of amyloid β (A β) plaques and the accumulation of phosphorylated tau protein as paired helical filaments within intraneuronal neurofibrillary tangles, as well as progressive neurodegeneration [1]. Progress has been made in identifying these neuropathological changes through cerebrospinal fluid (CSF) and positron emission tomography (PET) biomarkers, which classify patients using the amyloid/tau/neurodegeneration (AT(N)) biomarker system [2]. Three core CSF biomarkers including A β 42, phosphorylated

tau (p-tau) and total tau (t-tau), are believed to reflect amyloid pathology, tau pathology and neurodegeneration in AD [3–5]. However, these core CSF biomarkers represent just a fraction of the intricate pathophysiology underlying the disease, with AD also being characterized by dysfunction of multiple biological processes, such as synaptic transmission, mitochondrial metabolism and neuroinflammation [6]. There is thus urgent need for the identification of a diverse range of AD biomarkers to reflect these underlying pathological changes.

14–3-3 proteins are a family of conserved proteins that are ubiquitously expressed in various types of mammalian tissues, with the highest concentration of 14–3-3 proteins in brain tissue. There are seven known 14–3-3 isoforms: beta (β), gamma (γ), epsilon (ϵ), zeta (ζ), eta (η), theta

* Corresponding author.

E-mail address: hiadachi@med.uoeh-u.ac.jp (H. Adachi).

¹ Data used in preparation of this article were obtained from the Alzheimer's Disease Neuroimaging Initiative (ADNI) database (adni.loni.usc.edu). As such, the investigators within the ADNI contributed to the design and implementation of ADNI and/or provided data but did not participate in analysis or writing of this report. A complete listing of ADNI investigators can be found at: http://adni.loni.usc.edu/wp-content/uploads/how_to_apply/ADNI_Acknowledgement_List.pdf

<https://doi.org/10.1016/j.jns.2023.122861>

Received 12 May 2023; Received in revised form 3 December 2023; Accepted 27 December 2023

Available online 1 January 2024

0022-510X/© 2024 Elsevier B.V. All rights reserved.

(θ), and sigma (σ), and 14–3–3 zeta (ζ) is one of the isoforms encoded by the gene YWHAZ, which is located on the 8th chromosome in humans [7,8]. An earlier study reported that 14–3–3 ζ is present in neurofibrillary tangles of autopsied AD brains [9], and it has also been found that within the purified neurofibrillary tangles from AD brain extracts, 14–3–3 ζ interacts with tau protein [10]. Several studies have shown that 14–3–3 ζ binds to tau in the brain and promotes tau phosphorylation, mediates tau aggregation and causes synaptic pathology [11–14]. A recent study that utilized integrative proteomics to explore new CSF biomarkers related to AD identified hundreds of proteins that were significantly increased or decreased in AD patients. Among those altered proteins in the CSF samples of AD patients, CSF 14–3–3 ζ levels were increased [15]. Several studies have also reported CSF 14–3–3 ζ 's associations with AD [16,17].

The present study involved 719 participants from the Alzheimer's Disease Neuroimaging Initiative (ADNI) with available CSF 14–3–3 ζ measurements, who were cognitively normal (CN), or clinically diagnosed with mild cognitive impairment (MCI) or AD dementia. We aimed to identify whether CSF 14–3–3 ζ is associated with tau pathology and other CSF and blood biomarkers in AD, and the potential of CSF 14–3–3 ζ in predicting cognitive decline and disease progression.

2. Materials and methods

2.1. ADNI database

Funded as a public-private partnership project, the Alzheimer's disease Neuroimaging Initiative (ADNI) was launched in 2003 under the leadership of principal investigator Michael W. Weiner, MD. The primary goal of the ADNI project is to assess whether serial neuroimaging, and various clinical, biochemical, and genetic biomarkers can be combined to monitor progression of AD dementia. Data used in the preparation of this article were downloaded from the ADNI database (<http://adni.loni.usc.edu/>) in November 2021. This multi-centered research project was approved by regional ethical committees of all participating institutions, and all study procedures were performed in accordance with the principles of the Declaration of Helsinki. Informed consent was obtained from all study participants. From the ADNI, we included 719 participants with available CSF 14–3–3 ζ measurements. The study population was composed of CN participants and participants with clinically diagnosed MCI and AD dementia based on cognitive assessments. The inclusion and exclusion criteria, and the specific ADNI diagnostic criteria for distinguishing CN, MCI and AD participants have been described previously [18].

2.2. CSF 14–3–3 ζ measurements

CSF 14–3–3 ζ levels were measured by mass spectrometry using targeted proteomics assay at the Department of Neurology, Emory University School of Medicine. Crude CSF samples (50 μ L) from participants and quality control samples were reduced and alkylated by adding 5 mM TCEP, 40 mM chloroacetamide and 1% sodium deoxycholate in 100 mM triethylammonium bicarbonate buffer, then heated at 95 °C for 10 min followed by a 10 min cool down at room temperature. Digest solution (Lys-C and trypsin) was added to the CSF sample and left overnight at 37 °C. After digestion, isotopically labeled peptide standards for relative quantification were added to the peptide solution. The samples were desalted with 30-mg C18 HLB 96-well plates (Waters) according to the manufacturer's protocol, and eluates were dried using a vacuum.

For mass spectrometry analysis, samples were analyzed on a TSQ Altis Triple Quadrupole mass spectrometer (Thermo Fisher Scientific) fitted with an AdvanceBio Peptide analytical column and coupled to an Agilent 1290 Infinity II liquid chromatography system. The mass spectrometer was set to collect data in positive-ion mode using single reaction monitoring acquisition. The data obtained were subsequently uploaded into Skyline software for analysis. For each target analyte,

three transitions were acquired. The total area ratios for each peptide were calculated as follows: The area for each light (3) and heavy (3) transition was summed. The light total area was then divided by the heavy total area to obtain the total area ratios. Total area ratios were reported for relative quantification of the targeted peptide related to 14–3–3 ζ protein. Details of the targeted proteomics assay of CSF 14–3–3 ζ can be downloaded from the ADNI database (<http://adni.loni.usc.edu/>).

2.3. Cognitive assessments

The general cognition level of participants in the cohort was evaluated by the Mini-Mental State Examination (MMSE), the 11 item version of the Alzheimer's disease Assessment Scale Cognitive Subscale (ADAS-COG 11) and the CDR Scale Sum of Boxes (CDR-SB). Co-calibration of memory function, executive function and language function composite scores were generated using modern psychometric approaches across four cohorts: Alzheimer's Disease Neuroimaging Initiative (ADNI), Adult Changes in Thought (ACT), the Religious Orders Study and the Memory and Aging Project (ROS/MAP), and the National Alzheimer's Coordinating Center (NACC). The co-calibrated composite scores related to test results of memory function, executive function and language function are standardized on the same metric, which facilitate the composite scores in being comparable across different studies. All composite cognitive scores were downloaded from the dataset "ADSP Phenotype Harmonization Consortium (PHC)-Composite Cognitive Scores", and the detailed methods document applicable to this dataset is available from the ADNI database (<http://adni.loni.usc.edu/>).

2.4. CSF and plasma markers measurements

CSF samples were collected by lumbar puncture, and the method of lumbar puncture was described in the ADNI procedures manual (<http://www.adni-info.org/>). Levels of CSF A β 42, CSF total tau (t-tau), and CSF phosphorylated tau 181 (p-tau) were measured at the ADNI Biomarker Core laboratory at the University of Pennsylvania Medical Center using a fully automated Elecsys cobas e 601 instrument. CSF samples were analyzed using the electrochemiluminescence immunoassays (ECLIA) for Elecsys β -amyloid (1–42) CSF, phosphor-Tau (181P) CSF, and Total-Tau CSF according to the Roche Study Protocol and the kit manufacturer's instructions as previously described [19,20]. According to the ATN framework [2], the published cutoff values (CSF A β 42 < 977 pg/mL, CSF p-tau > 27 pg/mL, CSF t-tau > 300 pg/mL) were used to define amyloid pathology (A), tau pathology (T) and neurodegeneration (N) respectively [21]. CSF growth-associated protein 43 (GAP-43) levels were analyzed at the Clinical Neurochemistry Lab, University of Gothenburg, Sweden, by an in-house enzyme-linked immunosorbent assay (ELISA) method as previously described [22]. The ELISA was performed by combining mouse monoclonal GAP-43 antibody NM4 (coating antibody) (Fujirebio, Ghent, Belgium) and a polyclonal GAP-43 antibody (detector antibody) (ABB-135, Nordic Biosite, Sweden) that recognized the C-terminal of GAP-43.

Measurements of CSF soluble triggering receptor expressed on myeloid cells 2 (sTREM2) were analyzed with a Meso Scale Discovery (MSD) platform-based assay as previously reported [23], at Ludwig-Maximilians-Universität München, Munich, Germany. The MSD ELISA was conducted by combining the biotinylated polyclonal goat anti-human TREM2 antibody (capture antibody) (R&D Systems) that recognized aminoacids 19–174 of human TREM2 and the monoclonal mouse anti-human TREM2 antibody (detection antibody) (Santa Cruz Biotechnology) that recognized aminoacids 1–160 of human TREM2.

Plasma A β 42 and A β 40 levels were analyzed at Bateman lab, Washington University School of Medicine. Anti-A β mid-domain antibody (HJ5.1) was used to immunoprecipitate A β isoforms from plasma samples using a KingFisher (Thermo) automated immunoprecipitation platform, eluted A β species were subsequently digested with Lys-N protease then analyzed by liquid chromatography tandem mass

spectrometry (LC-MS/MS) as previously described [24]. Plasma p-tau181 and neurofilament light (NfL) levels were measured at the Clinical Neurochemistry Lab, University of Gothenburg, Sweden, using the Single Molecule array (Simoa) technique. The assay of plasma p-tau181 utilized a combination of two monoclonal antibodies (Tau12 and AT270) and measured N-terminal to mid-domain forms of p-tau181 [25]. Plasma NfL levels were measured using an NfL kit on a Simoa platform [26].

2.5. Neuroimaging

Structural MRI imaging in this study was performed using 3.0 T MRI scanners. Regional volume estimates were processed using FreeSurfer version 5.1 according to the 2010 Desikan-Killany atlas [27], and the input was T1 weighted MRI images in the NIfTI format. Hippocampus and medial temporal lobe data were used in our analyses, and intracranial volume was used to adjust for head size variation.

FDG-PET data were acquired according to the standardized protocol on the USC Laboratory of Neuroimaging (LONI) website (<https://adni.loni.usc.edu/>), and FDG-PET image data was processed by the Helen Wills Neuroscience Institute, University of California Berkeley and Lawrence Berkeley National Laboratory. For FDG-PET assessment, a composite ROI (region of interest) was generated by averaging across the left angular gyrus, right angular gyrus, bilateral posterior cingulate gyrus, left inferior temporal gyrus, right inferior temporal gyrus relative to the pons and cerebellar vermis reference regions [28].

2.6. Statistical analysis

According to the Shapiro-Wilk Test results and visual inspection of the histogram, the CSF 14–3–3 ζ data were found to be not normally distributed, thus the CSF 14–3–3 ζ data were log transformed to produce a normally distributed dataset. The differences of the log transformed CSF 14–3–3 ζ biomarker between two groups were compared by two sample *t*-tests, and differences across multiple groups were examined with one-way analysis of variance (ANOVA) and the Tukey post hoc test. To investigate differences across multiple groups while adjusting for potential confounders, we employed an Analysis of Covariance (ANCOVA) that incorporated age, sex, education years, and APOE4 status as covariates. Significant differences between the groups were

further explored using the Tukey post hoc test. Receiver operating characteristic (ROC) analyses were used to evaluate the diagnostic accuracy of CSF 14–3–3 ζ , the specificity and sensitivity of CSF 14–3–3 ζ were determined based on area under the curve (AUC) analyses. For the comparison of the predictive accuracy of CSF 14–3–3 ζ , CSF p-tau, and the different models for clinical conversion from MCI to AD dementia, analyses were conducted using Generalized Estimating Equations (GEE) with a binomial outcome representing conversion to AD dementia from MCI. The selected GEE model featured an exchangeable correlation structure and robust standard errors. ROC curves were employed to compare the predictive accuracy of the various biomarkers and models. The plot to predict probability of tau positive status based on CSF 14–3–3 ζ levels was created using marginsplot code in Stata software. Associations between the other biofluid markers with CSF 14–3–3 ζ were tested by linear regression models with adjustment for age, sex, years of education and APOE ϵ 4 status. Longitudinal analysis of the changes of cognition scores and neuroimaging findings over time in different CSF 14–3–3 ζ level groups (stratified into low, intermediate and high levels) were conducted using linear mixed-effect models (LME). All LME models included interaction between time and group with random intercepts and slopes, and unstructured covariance structure for random effects. All LME models were adjusted for age, sex, years of education and APOE ϵ 4 status, and models involving MRI imaging of brain structures were also adjusted for intracranial volume. We derived participant-specific slopes for the MMSE, ADAS-COG 11, hippocampus, and FDG-PET measures. For the cognitive scores (MMSE and ADAS-COG 11), participant-specific linear regression models were employed, using longitudinal cognitive scores as outcomes and time (years since baseline) as the predictor. Similarly, for the neuroimaging measures (hippocampus and FDG-PET), we used participant-specific linear regression models with the respective longitudinal neuroimaging data as outcomes and time as the predictor. Each participant's data required at least two time points for model fitting. The participant-specific slopes derived from these models were subsequently used as outcomes in a secondary set of linear regression models with individual biomarkers as predictors, adjusted for age, sex, years of education, APOE ϵ 4 status, and the respective baseline cognitive scores or neuroimaging findings. For comparative purposes, basic models were also fitted using only the covariates (age, sex, years of education, APOE ϵ 4 status) without the biomarkers. Statistical analyses were performed using Stata version 16 (College Station, TX) statistical

Table 1

Baseline demographic characteristics of the study population.

Variable	CN (<i>n</i> = 225)	MCI (<i>n</i> = 381)	AD (<i>n</i> = 113)	<i>P</i> -value
Age at baseline, years	73.06 (6.06)	71.17 (7.58)	74.27 (8.34)	<0.001
Male sex, N (%)	99 (44.00%)	208 (54.59%)	68 (60.18%)	0.007
Education level, years	16.64 (2.51)	16.24 (2.62)	15.74 (2.70)	0.011
APOE ϵ 4 status, N (%)				<0.001
APOE ϵ 4–/–, N (%)	161 (71.56%)	196 (51.44%)	38 (33.63%)	
APOE ϵ 4+/-, N (%)	57 (25.33%)	145 (38.06%)	50 (44.25%)	
APOE ϵ 4+/+, N (%)	7 (3.11%)	40 (10.50%)	25 (22.12%)	
CSF biomarkers				
A β 42 level, pg/mL	1033.23 (377.47)	896.32 (335.18)	648.68 (259.78)	<0.001
p-tau level, pg/mL	21.73 (9.53)	26.10 (14.10)	37.48 (16.15)	<0.001
t-tau level, pg/mL	236.43 (93.60)	272.38 (125.99)	378.29 (153.65)	<0.001
14–3–3 ζ , total_area_ratio	0.023 (0.009)	0.026 (0.011)	0.033 (0.011)	<0.001
Neuroimaging ^a				
Hippocampus, mm ³	7530.92 (881.47)	7072.44 (1120.39)	5957.63 (916.30)	<0.001
Medial temporal lobe, mm ³	20,747.76 (2517.69)	20,391.78 (2717.59)	17,807.44 (3245.54)	<0.001
FDG-PET composite	1.32 (0.11)	1.26 (0.14)	1.06 (0.15)	<0.001
Cognitive score				
MEM composite	0.89 (0.47)	0.27 (0.54)	–0.78 (0.33)	<0.001
EXF composite	0.74 (0.48)	0.42 (0.54)	–0.38 (0.68)	<0.001
LAN composite	0.79 (0.48)	0.46 (0.49)	–0.19 (0.56)	<0.001

Continuous variables are reported as means (standard deviations), and categorical variables are reported as numbers and percentages.

Abbreviations: CSF, cerebrospinal fluid; p-tau, phosphorylated tau 181; t-tau, total tau; FDG-PET, fluorodeoxyglucose-positron emission tomography; MEM, memory function; EXF, executive function; LAN, language function.

^a MRI imaging measurements are not adjusted by total intracranial volume.

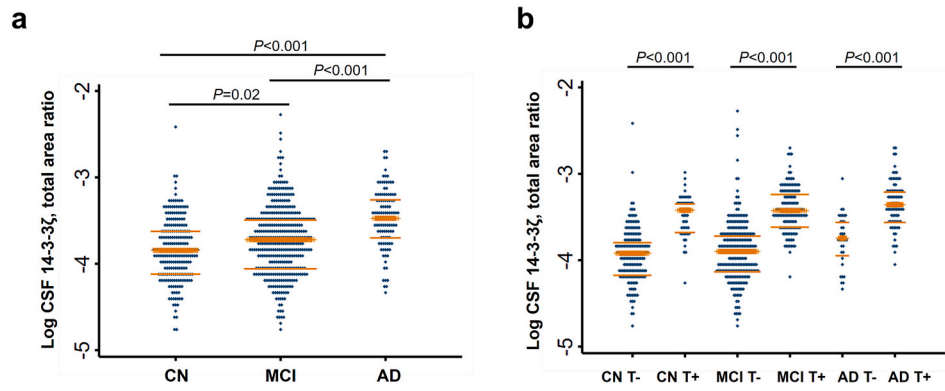


Fig. 1. Raw CSF 14–3–3 ζ concentrations in different diagnostic groups.

a, CSF 14–3–3 ζ concentrations in cognitively normal (CN) participants, individuals with mild cognitive impairment (MCI) and Alzheimer's disease (AD) dementia. b, CSF 14–3–3 ζ concentrations in CN, MCI and AD dementia groups with tau negative (T-) and tau positive (T+) statuses respectively. T indicates tau pathology, the positivity of tau pathology was defined by the published cutoff value (CSF p-tau >27 pg/mL). Differences across groups were examined with one-way ANOVA and the Tukey post hoc test. The significant differences between groups have been validated even after adjustments for potential confounders. Refer to Supplementary Fig. 1 for the adjusted means plot.

software and R (version 4.2.0), and two-sided $P < 0.05$ was considered statistically significant.

3. Results

We studied 719 participants in the cohort with available baseline CSF 14–3–3 ζ measurements. Of the 719 participants included in this study, 225 were CN controls, 381 had MCI, and 113 had AD dementia, further demographic characteristics according to clinical diagnosis are shown in Table 1. Fig. 1a illustrates the CSF 14–3–3 ζ measured in the CN, MCI and AD dementia groups. CSF 14–3–3 ζ levels were increased in the AD dementia group compared with the other clinical diagnostic groups

($P < 0.001$). CSF 14–3–3 ζ concentrations in participants with MCI were higher than CN controls ($P = 0.02$). Groups were further stratified according to participant characteristics including clinical diagnosis and CSF tau status, and the tau positive clinical diagnostic groups had higher CSF 14–3–3 ζ levels than their counterpart tau negative groups ($P < 0.001$) (Fig. 1b). After adjusting for age, sex, education years, and APOE4 status, these differences remained significant (Supplementary Fig. 1).

We evaluated the association of CSF 14–3–3 ζ levels with tau pathology as measured by CSF p-tau and plasma p-tau, and CSF 14–3–3 ζ levels were positively associated with CSF p-tau ($r = 0.741, P < 0.001$) (Fig. 2a) and plasma p-tau ($r = 0.293, P < 0.001$) (Fig. 2b). The

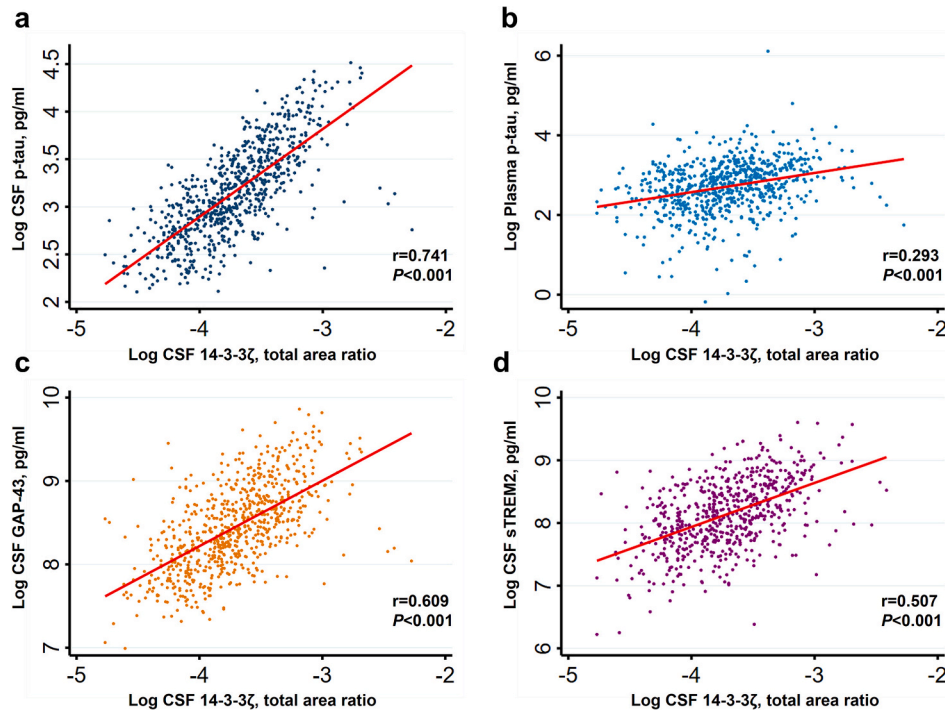


Fig. 2. Association between CSF 14–3–3 ζ and other fluid biomarkers of AD.

a-d. Scatter plots representing the associations of CSF 14–3–3 ζ with other AD fluid biomarkers. a-b. CSF 14–3–3 ζ was positively correlated with CSF p-tau and plasma p-tau in this cohort. c. CSF 14–3–3 ζ was positively correlated with synaptic biomarker CSF GAP-43 d. CSF 14–3–3 ζ was positively correlated with neuroinflammatory biomarker CSF sTREM2. Associations between log transformed fluid biomarkers were demonstrated as fit lines in the cohort and assessed by Pearson correlation. Abbreviations: CSF, cerebrospinal fluid; p-tau, phosphorylated tau 181; GAP-43, growth-associated protein 43; sTREM2, soluble triggering receptor expressed on myeloid cells 2.

Table 2
Associations between CSF 14–3–3 ζ and other fluid biomarkers of AD.

Biomarker	CSF 14–3–3 ζ			
	β -coefficient	P-value	P_{adj} value	R ²
CSF A β 42	–0.055	0.223	0.260	0.114
CSF p-tau	0.690	<0.001	<0.001	0.513
CSF t-tau	0.704	<0.001	<0.001	0.535
CSF GAP-43	0.484	<0.001	<0.001	0.326
CSF sTREM2	0.443	<0.001	<0.001	0.293
Plasma A β 42/40	–0.049	0.442	0.442	0.052
Plasma p-tau	0.119	0.001	0.002	0.121
Plasma NFL	0.111	0.005	0.007	0.118

Linear regression models were used to examine associations between CSF 14–3–3 ζ and other fluid biomarkers (all fluid biomarkers were standardized to z scores), adjusted for age, sex, education years, and APOE ϵ 4 genotype. P_{adj} represents P-values that were corrected for multiple comparisons with the Benjamini-Hochberg method. Abbreviations: CSF, cerebrospinal fluid; p-tau, phosphorylated tau 181; t-tau, total tau; NFL, neurofilament light; GAP-43, growth-associated protein 43; sTREM2, soluble triggering receptor expressed on myeloid cells 2.

participants were further stratified by clinical diagnostic group, and CSF 14–3–3 ζ levels were positively associated with CSF p-tau in all diagnostic groups (Supplementary Fig. 2). CSF 14–3–3 ζ levels were also positively associated with the synaptic biomarker CSF GAP-43 ($r = 0.609$, $P < 0.001$) (Fig. 2c) and neuroinflammatory biomarker CSF sTREM-2 ($r = 0.507$, $P < 0.001$) (Fig. 2d). In our linear regression analyses, we observed no significant interactions between tau status with either CSF GAP-43 ($\beta = 0.075$, $P = 0.318$) or CSF sTREM2 ($\beta = 0.016$, $P = 0.813$) (Supplementary Fig. 3). These findings suggest that the relationships between CSF 14–3–3 ζ and both CSF GAP-43 and CSF sTREM2 remain consistent regardless of tau status. There were no associations of CSF 14–3–3 ζ levels with CSF A β 42, or plasma A β 42/40 ratios (Table 2).

As illustrated in Fig. 3a, CSF 14–3–3 ζ levels were higher in tau

pathology positive participants compared with tau pathology negative participants ($P < 0.0001$), tau pathology statuses were defined by CSF p-tau. We next investigated how CSF 14–3–3 ζ levels discriminate tau status by using ROC analysis, and CSF 14–3–3 ζ as a biomarker could accurately discriminate tau positive participants from tau negative participants, with an area under the curve (AUC) of 0.891 (Fig. 3b). A plot was constructed to estimate the probability of positive tau status based on a participant's CSF 14–3–3 ζ levels, which indicated that CSF 14–3–3 ζ levels are a strong predictor for tau status (Fig. 3c). We compared the predictive accuracy of CSF 14–3–3 ζ , CSF p-tau, the CSF 14–3–3 ζ model (which incorporated CSF 14–3–3 ζ , age, sex, education years, and APOE ϵ 4 genotype), and the combined model (which incorporated CSF 14–3–3 ζ , CSF p-tau, age, sex, education years, and APOE ϵ 4 genotype) for the

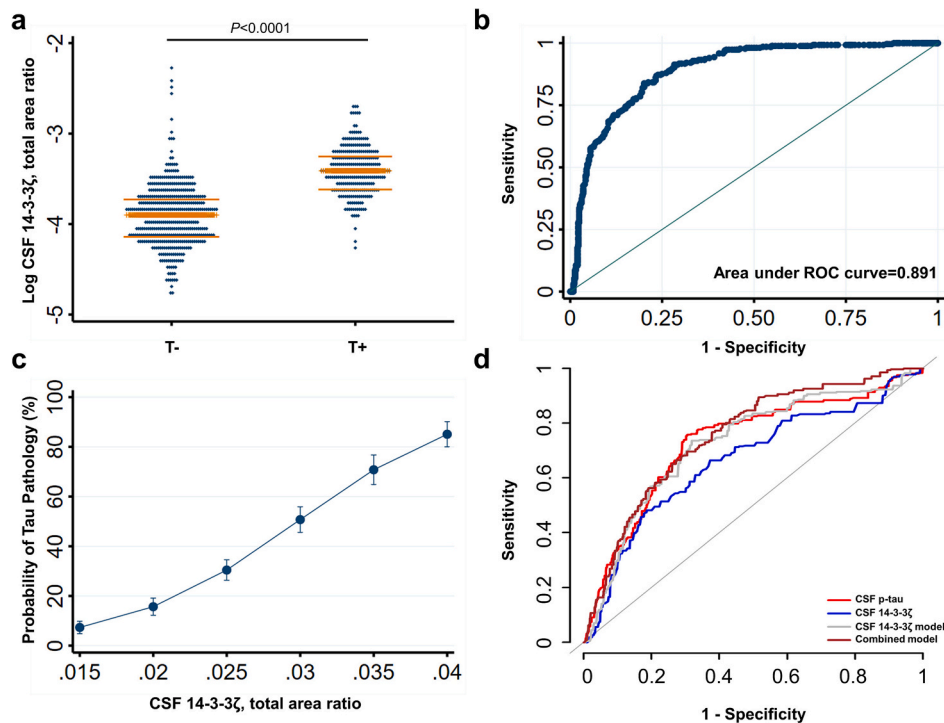


Fig. 3. CSF 14–3–3 ζ concentration according to tau pathology positivity.

a, CSF 14–3–3 ζ concentration in tau negative and tau positive participants. b, Receiver operating characteristic (ROC) analyses of CSF 14–3–3 ζ for distinguishing positive and negative tau pathology status. c, Prediction of tau pathology probability by CSF 14–3–3 ζ concentration. d, ROC curves illustrating the predictive accuracy for clinical conversion from MCI to AD dementia. The curves represent the following biomarkers and models: CSF p-tau (red line, AUC = 0.732), CSF 14–3–3 ζ (blue line, AUC = 0.665), the CSF 14–3–3 ζ model which included CSF 14–3–3 ζ , age, sex, education years, and APOE ϵ 4 genotype (grey line, AUC = 0.726), and the combined model which included CSF 14–3–3 ζ , CSF p-tau, age, sex, education years, and APOE ϵ 4 genotype (brown line, AUC = 0.754). The accuracy comparisons are based on the DeLong test. Tau pathology positivity was defined by the published cutoff value as CSF p-tau >27 pg/mL. Abbreviations: AUC, area under the curve; AD, Alzheimer's disease; MCI, mild cognitive impairment; CSF, cerebrospinal fluid; p-tau, phosphorylated tau 181. (For interpretation of the references to colour in this figure legend, the reader is referred to the web version of this article.)

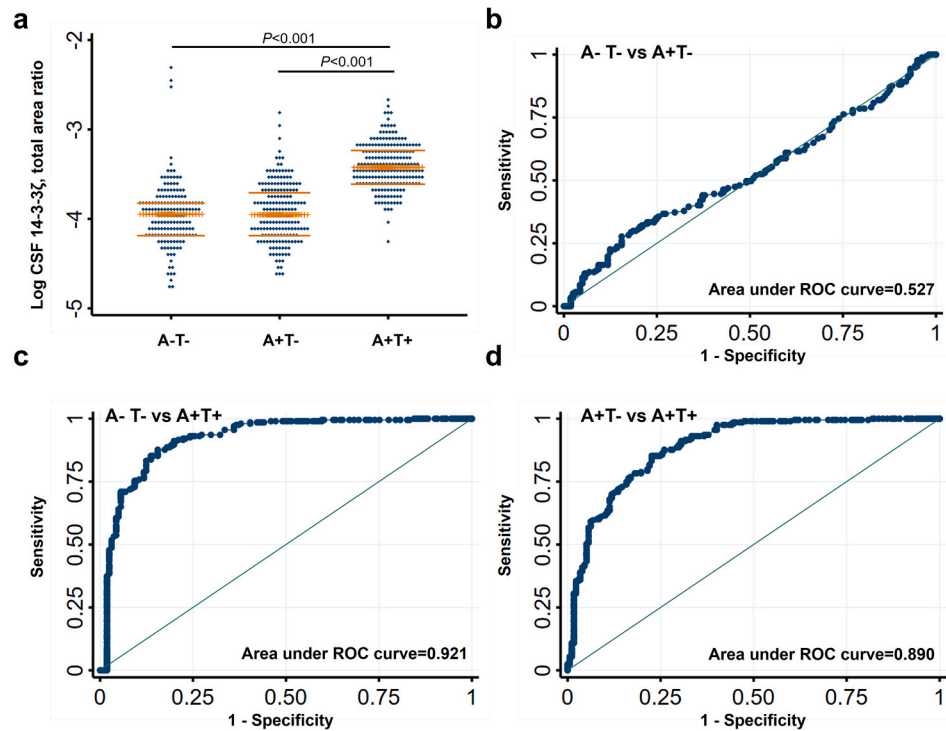


Fig. 4. CSF 14-3-3 ζ concentration according to amyloid and tau status.

a, CSF 14-3-3 ζ concentrations in participants according to A β /tau (AT) profile. b, Receiver operating characteristic (ROC) analyses of CSF 14-3-3 ζ for distinguishing A-T- from A + T-. c, ROC analyses of CSF 14-3-3 ζ for distinguishing A-T- from A + T+. d, ROC analyses of CSF 14-3-3 ζ for distinguishing A + T- from A + T+. A indicates amyloid pathology, T indicates tau pathology, and the cutoff values (CSF A β 42 < 977 pg/mL, CSF p-tau > 27 pg/mL) were used to define the positivity of amyloid pathology and tau pathology respectively.

clinical conversion from MCI to AD dementia. The accuracy of CSF p-tau (AUC = 0.732) was comparable to the CSF 14-3-3 ζ model (AUC = 0.726; DeLong P = 0.387) and the combined model (AUC = 0.754; DeLong P = 0.099), and was significantly higher than that of CSF 14-3-3 ζ alone (AUC = 0.665; DeLong P < 0.001) (Fig. 3d).

We further utilized the CSF biomarker based amyloid pathology (A), tau pathology (T) classification (AT classification), which classified the participants into three groups: A β - and tau- (A-T-), A β + but tau- (A + T-) and A β + and tau+ (A + T+). CSF 14-3-3 ζ levels were significantly higher in the A + T+ group than the other two groups (P < 0.001), and there were no statistically significant differences between the A-T- and A + T- groups (Fig. 4a). We conducted ROC analysis to determine the ability of CSF 14-3-3 ζ to discriminate between different AT groups. CSF 14-3-3 ζ distinguished the A-T- group from the A + T+ group (AUC = 0.921, Fig. 4c), but not from the A + T- group (AUC = 0.527, Fig. 4b). CSF 14-3-3 ζ also distinguished the A + T- group from the A + T+ group (AUC = 0.890, Fig. 4d).

Based on tertiles of CSF 14-3-3 ζ levels distribution, we subdivided the participants into low level, intermediate level and high level groups. Fig. 5 shows associations of baseline and longitudinal cognition and neuroimaging findings with CSF 14-3-3 ζ levels (Supplementary Table 1-6 listed coefficients and P -values). At baseline, high and intermediate levels of CSF 14-3-3 ζ were associated with worse memory and language function. High levels of CSF 14-3-3 ζ were associated with reductions in executive function, lower FDG-PET values, and smaller hippocampus and medial temporal lobe volumes. Over time, high and intermediate CSF 14-3-3 ζ levels were associated with more rapid decline of memory, executive and language function, and accelerated reduction in hippocampus volumes and FDG-PET values. High CSF 14-3-3 ζ levels were associated with a faster reduction in medial temporal lobe volume during follow up. After adjusting for covariates, our examination of selected CSF biomarkers revealed that CSF p-tau was significantly associated with all longitudinal cognitive and

neuroimaging measures, including MMSE, ADAS-COG 11, hippocampus volume, and FDG-PET slopes. Similarly, CSF 14-3-3 ζ consistently exhibited significance across these evaluations. While CSF p-tau emerged as a stronger predictor of cognitive and neurodegenerative trajectories, CSF 14-3-3 ζ 's performance was notably robust when compared to the other CSF biomarkers in terms of R^2 values (MMSE: R^2 = 0.148, P < 0.001; ADAS-COG 11: R^2 = 0.099, P = 0.001; Hippocampus volume: R^2 = 0.052, P = 0.002; FDG-PET: R^2 = 0.099, P < 0.001) (Supplementary Tables 7-10). Furthermore, we have compared the Akaike Information Criterion (AIC) across several models: the covariates-only model (which included age, sex, years of education, and APOE ϵ 4 genotype), the p-tau model (which included CSF p-tau in addition to the covariates), the 14-3-3 ζ model (which included CSF 14-3-3 ζ and the covariates), and the combined model (which included both CSF p-tau and CSF 14-3-3 ζ , as well as the covariates) for predicting cognition and neuroimaging slopes. Our comparisons revealed that for predicting MMSE slopes, the best model (the model with the lowest AIC) is the combined model (AIC for the model: 2903.02). Similarly, for FDG-PET, the combined model again proved to be the best model (AIC for the model: -1280.85). These findings suggest that the combination of CSF p-tau and CSF 14-3-3 ζ biomarkers provides better predictions in these contexts. However, for the ADAS-COG11 and hippocampus volume, the p-tau model was superior (For ADAS-COG11, AIC: 3910.78; For hippocampus volume, AIC: 8828.98), indicating that the addition of CSF 14-3-3 ζ does not enhance the model's predictive power for these particular outcomes (Supplementary Tables 7-10).

4. Discussion

In this study we demonstrated that CSF 14-3-3 ζ was increased in AD, with the increase seemingly attributed to individuals positive for tau pathology. We also found that CSF 14-3-3 ζ was correlated to fluid biomarkers of tau pathology, as well as fluid biomarkers of synaptic

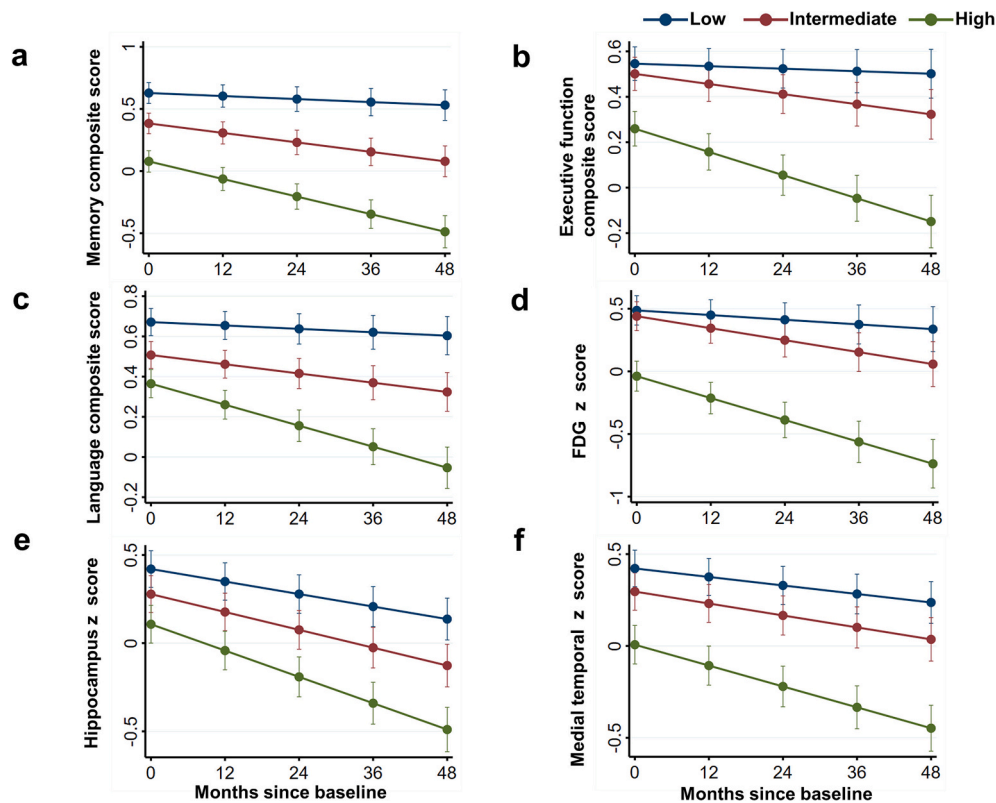


Fig. 5. Associations between baseline CSF 14-3-3 ζ levels, cognitive function, and neuroimaging findings over time.

CSF 14-3-3 ζ levels were categorized into three tertiles: Low, Intermediate, and High. The figure shows trajectories of co-calibrated cognitive composite scores for memory (a), executive function (b), and language (c), as well as neuroimaging z scores for FDG-PET values (d), hippocampus volumes (e), and medial temporal region volumes (f). These cognitive composite scores, sourced from the ADSP Phenotype Harmonization Consortium, were harmonized across various cohorts. The trajectories were tested in linear mixed-effects regression models, adjusted for age, sex, education years, and APOE ϵ 4 genotype, as well as intracranial volume for the MRI structural measurements.

dysfunction and neuroinflammation. Furthermore, we have shown that CSF 14-3-3 ζ had good diagnostic accuracy in distinguishing tau pathology statuses, and was associated with progressive decline of cognitive function and neuroimaging findings during follow up. The current investigation provides substantial evidence regarding the clinical significance of CSF 14-3-3 ζ as a potential biomarker for AD. Notably, our findings provide a strong basis for understanding the relationships between CSF 14-3-3 ζ levels and several other diagnostic and pathological markers of AD.

Our study showed elevated CSF 14-3-3 ζ levels among the AD dementia group compared to the CN controls and those with MCI. This elevation further reinforces the possible role of CSF 14-3-3 ζ in the pathogenesis of AD. Moreover, the concentration differences between MCI and CN controls indicate its potential use as an early-stage diagnostic tool.

Since hyperphosphorylated tau protein and 14-3-3 ζ are components of neurofibrillary tangles, there might also be a correlation between 14-3-3 ζ released in CSF and the extent of neurofibrillary tangle pathology in the brain. Our study demonstrated that CSF 14-3-3 ζ levels were correlated to CSF p-tau and plasma p-tau levels. Since CSF p-tau and plasma p-tau are believed to reflect tau pathology in AD [2,25], our findings suggest that CSF 14-3-3 ζ levels were associated with tau pathology. Furthermore, CSF 14-3-3 ζ was particularly pronounced in tau pathology positive participants compared to negative participants, and CSF 14-3-3 ζ could efficiently distinguish tau pathology status (AUC = 0.891). In this study, A + T- indicated a status of amyloid pathological change, and A + T+ represented an advanced pathological stage with both amyloid and tau pathologies present. CSF 14-3-3 ζ could effectively discriminate between A + T- and A + T+ stages (AUC = 0.890), indicating that CSF 14-3-3 ζ as a biomarker was associated with tau

pathology and had good performance in identifying an advanced AD pathological stage.

In this study we observed that CSF 14-3-3 ζ levels were associated with CSF GAP-43 and CSF sTREM2. GAP-43 is a protein located on the cytoplasmic side of the presynaptic membrane [29], and studies have indicated that CSF GAP-43 is a biomarker of synaptic dysfunction in AD [22,30,31]. In the central nervous system, TREM2 is an immune receptor located in the plasma membrane of microglia, microglial cell surface TREM2 can be shed by proteases, which then releases soluble TREM2 (sTREM2) into biological fluid such as the CSF and blood [32,33]. sTREM2 in CSF can be considered as a microglial and neuro-inflammatory biomarker of AD [34]. Our findings suggest the combination of synaptic dysfunction, microglial activation and 14-3-3 ζ pathological changes in AD.

Our study also compared the strength of association between CSF 14-3-3 ζ and tau pathology to that of other known biomarkers, revealing a significant correlation between CSF 14-3-3 ζ and both tau proteins (p-tau and t-tau) with R^2 values of 0.513 and 0.535, respectively. These findings indicate that CSF 14-3-3 ζ is a robust correlate of tau pathology, and the mechanisms underlying this association require further investigation. While plasma biomarkers like plasma p-tau and plasma NfL also correlated with CSF 14-3-3 ζ , their associations were moderate. Collectively, these findings underscore the role of CSF 14-3-3 ζ in the complex landscape of AD.

Another finding of this study was that CSF 14-3-3 ζ levels were associated with cognitive decline and neuroimaging measures at baseline and over time. In terms of cognitive decline, CSF 14-3-3 ζ levels were significantly associated with declined memory, language, and executive functions longitudinally. For neuroimaging measures, longitudinal associations between CSF 14-3-3 ζ levels and decreased FDG

metabolism, hippocampus and medial temporal volumes were observed. An increase in CSF 14–3–3 ζ that was associated with worsening cognition and brain atrophy over time suggests that baseline CSF 14–3–3 ζ levels could be used as a biomarker to predict progression of cognitive decline and worsening neuroimaging findings in AD patients. From our analysis, it appears that while CSF 14–3–3 ζ might not be superior to CSF p-tau in terms of predicting cognitive outcomes and neuroimaging findings, it does have advantages over other CSF biomarkers (such as CSF sTREM2, CSF GAP-43) in terms of predictability. This suggests that CSF 14–3–3 ζ might provide added value in certain contexts or when used in combination with other biomarkers. From a practical perspective, if 14–3–3 ζ is more accessible, less expensive, or easier to measure than CSF p-tau, it might be a valuable addition to clinical assessments, especially in settings where resources are limited.

The present study has several limitations. First, this study lacked inclusion of participants with other neurodegenerative diseases besides AD, which limits our ability to investigate whether CSF 14–3–3 ζ is associated with the neuropathological biomarkers of those disorders, such as α -synuclein in Parkinson's disease and TDP-43 in amyotrophic lateral sclerosis. Second, another limitation is that this study lacks tau-PET measurements, in this study CSF p-tau and plasma p-tau were used as proxies in the assessment of tau pathology, however a previous study demonstrated that tau-PET imaging was associated with tau pathology more closely compared to fluid biomarkers [35]. Third, in this study we mainly used CSF phosphorylated tau 181 to define tau pathology, and the other tau phosphorylation sites such as CSF phosphorylated tau 217 may perform better than CSF phosphorylated tau 181 [36,37]. Finally, our study lacked longitudinal CSF 14–3–3 ζ data, and analyzing longitudinal changes of CSF 14–3–3 ζ levels could better delineate the characteristics of CSF 14–3–3 ζ in AD.

5. Conclusion

In the present study, our results suggest that CSF 14–3–3 ζ is a novel biomarker of tau pathology and neurodegeneration in AD. Given its strong association with tau pathology, along with its association with cognitive function, further research is warranted. While CSF p-tau remains a potent predictor for AD progression, CSF 14–3–3 ζ 's performance, especially compared to other CSF biomarkers, underlines its clinical importance. As a biomarker, CSF 14–3–3 ζ could be used to predict cognitive decline and disease progression in clinical practice and in AD clinical trials.

Declaration of competing interest

The authors declare that there are no known competing financial interests or personal relationships which could have been perceived as influencing the work presented in this paper.

Data availability

Data utilized in the present study were originally downloaded from the online repository of Alzheimer's Disease Neuroimaging Initiative (ADNI) (<http://adni.loni.usc.edu/>).

Acknowledgements

The authors express their appreciation to the Alzheimer's Disease Neuroimaging Initiative (ADNI) study. Data utilized in the preparation of this manuscript were obtained from the ADNI database (<http://adni.loni.usc.edu/>), data collection and sharing for this project was funded by the ADNI (National Institutes of Health Grant U01 AG024904) and DOD ADNI (Department of Defense award number W81XWH-12-2-0012). ADNI is funded by the National Institute on Aging, the National Institute

of Biomedical Imaging and Bioengineering, and through generous contributions from the following: AbbVie, Alzheimer's Association; Alzheimer's Drug Discovery Foundation; Araclon Biotech; BioClinica, Inc.; Biogen; Bristol-Myers Squibb Company; CereSpir, Inc.; Cogstate; Eisai Inc.; Elan Pharmaceuticals, Inc.; Eli Lilly and Company; EuroImmun; F. Hoffmann-La Roche Ltd. and its affiliated company Genentech, Inc.; Fujirebio; GE Healthcare; IXICO Ltd.; Janssen Alzheimer Immunotherapy Research & Development, LLC; Johnson & Johnson Pharmaceutical Research & Development LLC; Lumosity; Lundbeck; Merck & Co., Inc.; Meso Scale Diagnostics, LLC; NeuroRx Research; Neurotrack Technologies; Novartis Pharmaceuticals Corporation; Pfizer Inc.; Piramal Imaging; Servier; Takeda Pharmaceutical Company; and Transition Therapeutics. The Canadian Institutes of Health Research is providing funds to support ADNI clinical sites in Canada. Private sector contributions are facilitated by the Foundation for the National Institutes of Health (www.fnih.org). The grantee organization is the Northern California Institute for Research and Education, and the study is coordinated by the Alzheimer's Therapeutic Research Institute at the University of Southern California. ADNI data are disseminated by the Laboratory for Neuro Imaging at the University of Southern California.

Appendix A. Supplementary data

Supplementary data to this article can be found online at <https://doi.org/10.1016/j.jns.2023.122861>.

References

- [1] T.J. Montine, C.H. Phelps, T.G. Beach, E.H. Bigio, N.J. Cairns, D.W. Dickson, C. Duyckaerts, M.P. Frosch, E. Masliah, S.S. Mirra, P.T. Nelson, J.A. Schneider, D. R. Thal, J.Q. Trojanowski, H.V. Vinters, B.T. Hyman, A. National Institute on, A. Alzheimer's, National Institute on Aging-Alzheimer's Association guidelines for the neuropathologic assessment of Alzheimer's disease: a practical approach, *Acta Neuropathol.* 123 (1) (2012) 1–11.
- [2] C.R. Jack Jr., D.A. Bennett, K. Blennow, M.C. Carrillo, B. Dunn, S.B. Haeberlein, D. M. Holtzman, W. Jagust, F. Jessen, J. Karlawish, E. Liu, J.L. Molinuevo, T. Montine, C. Phelps, K.P. Rankin, C.C. Rowe, P. Scheltens, E. Siemers, H.M. Snyder, R. Sperling, NIA-AA research framework: toward a biological definition of Alzheimer's disease, *Alzheimers Dement.* 14 (4) (2018) 535–562.
- [3] K. Blennow, H. Hampel, M. Weiner, H. Zetterberg, Cerebrospinal fluid and plasma biomarkers in Alzheimer disease, *Nat. Rev. Neurol.* 6 (3) (2010) 131–144.
- [4] N.J. Ashton, M. Scholl, K. Heurling, E. Gkanatsiou, E. Portelius, K. Hoglund, G. Brinkmalm, A. Hye, K. Blennow, H. Zetterberg, Update on biomarkers for amyloid pathology in Alzheimer's disease, *Biomark. Med* 12 (7) (2018) 799–812.
- [5] M. Scholl, A. Maass, N. Mattsson, N.J. Ashton, K. Blennow, H. Zetterberg, W. Jagust, Biomarkers for tau pathology, *Mol. Cell. Neurosci.* 97 (2019) 18–33.
- [6] B. De Strooper, E. Karran, The cellular phase of Alzheimer's disease, *Cell* 164 (4) (2016) 603–615.
- [7] D. Berg, C. Holzmann, O. Riess, 14-3-3 proteins in the nervous system, *Nat. Rev. Neurosci.* 4 (9) (2003) 752–762.
- [8] M. Foote, Y. Zhou, 14-3-3 proteins in neurological disorders, *Int J Biochem Mol Biol* 3 (2) (2012) 152–164.
- [9] T. Umahara, T. Uchihara, K. Tsuchiya, A. Nakamura, T. Iwamoto, K. Ikeda, M. Takasaki, 14-3-3 proteins and zeta isoform containing neurofibrillary tangles in patients with Alzheimer's disease, *Acta Neuropathol.* 108 (4) (2004) 279–286.
- [10] H.Y. Qureshi, T. Li, R. MacDonald, C.M. Cho, N. Leclerc, H.K. Paudel, Interaction of 14-3-3zeta with microtubule-associated protein tau within Alzheimer's disease neurofibrillary tangles, *Biochemistry* 52 (37) (2013) 6445–6455.
- [11] M. Hashiguchi, K. Sobue, H.K. Paudel, 14-3-3zeta is an effector of tau protein phosphorylation, *J. Biol. Chem.* 275 (33) (2000) 25247–25254.
- [12] T. Li, H.K. Paudel, 14-3-3zeta facilitates GSK3 β -catalyzed tau phosphorylation in HEK-293 cells by a mechanism that requires phosphorylation of GSK3 β on Ser9, *Neurosci. Lett.* 414 (3) (2007) 203–208.
- [13] H.Y. Qureshi, D. Han, R. MacDonald, H.K. Paudel, Overexpression of 14-3-3zeta promotes tau phosphorylation at Ser262 and accelerates proteasomal degradation of synaptophysin in rat primary hippocampal neurons, *PLoS One* 8 (12) (2013) e84615.
- [14] T. Li, H.K. Paudel, 14-3-3zeta mediates tau aggregation in human neuroblastoma M17 cells, *PLoS One* 11 (8) (2016) e0160635.
- [15] L. Higginbotham, L. Ping, E.B. Dammer, D.M. Duong, M. Zhou, M. Gearing, C. Hurst, J.D. Glass, S.A. Factor, E.C.B. Johnson, I. Hajjar, J.J. Lah, A.I. Levey, N. T. Seyfried, Integrated proteomics reveals brain-based cerebrospinal fluid biomarkers in asymptomatic and symptomatic Alzheimer's disease, *Sci. Adv.* 6 (43) (2020).
- [16] Q. Gu, E. Cuevas, J. Raymick, J. Kanungo, S. Sarkar, Downregulation of 14-3-3 proteins in Alzheimer's disease, *Mol. Neurobiol.* 57 (1) (2020) 32–40.

- [17] Y. Lu, Early increase of cerebrospinal fluid 14-3-3zeta protein in the alzheimer's disease continuum, *Front. Aging Neurosci.* 14 (2022) 941927.
- [18] R.C. Petersen, P.S. Aisen, L.A. Beckett, M.C. Donohue, A.C. Gamst, D.J. Harvey, C. R. Jack Jr., W.J. Jagust, L.M. Shaw, A.W. Toga, J.Q. Trojanowski, M.W. Weiner, Alzheimer's disease neuroimaging initiative (ADNI): clinical characterization, *Neurology* 74 (3) (2010) 201–209.
- [19] T. Bittner, H. Zetterberg, C.E. Teunissen, R.E. Ostlund Jr., M. Militello, U. Andreasson, I. Hubeek, D. Gibson, D.C. Chu, U. Eichenlaub, P. Heiss, U. Kobold, A. Leinenbach, K. Madin, E. Manuilova, C. Rabe, K. Blennow, Technical performance of a novel, fully automated electrochemiluminescence immunoassay for the quantitation of beta-amyloid (1-42) in human cerebrospinal fluid, *Alzheimers Dement.* 12 (5) (2016) 517–526.
- [20] O. Hansson, J. Seibyl, E. Stomrud, H. Zetterberg, J.Q. Trojanowski, T. Bittner, V. Lifke, V. Corradini, U. Eichenlaub, R. Batrla, K. Buck, K. Zink, C. Rabe, K. Blennow, L.M. Shaw, F.S.G. Swedish Bio, I. Alzheimer's Disease Neuroimaging, CSF biomarkers of Alzheimer's disease concord with amyloid-beta PET and predict clinical progression: a study of fully automated immunoassays in BioFINDER and ADNI cohorts, *Alzheimers Dement.* 14 (11) (2018) 1470–1481.
- [21] K. Blennow, L.M. Shaw, E. Stomrud, N. Mattsson, J.B. Toledo, K. Buck, S. Wahl, U. Eichenlaub, V. Lifke, M. Simon, J.Q. Trojanowski, O. Hansson, Predicting clinical decline and conversion to Alzheimer's disease or dementia using novel Elecsys Abeta(1-42), pTau and tTau CSF immunoassays, *Sci. Rep.* 9 (1) (2019) 19024.
- [22] A. Sandelius, E. Portelius, A. Kallen, H. Zetterberg, U. Rot, B. Olsson, J.B. Toledo, L. M. Shaw, V.M.Y. Lee, D.J. Irwin, M. Grossman, D. Weintraub, A. Chen-Plotkin, D. A. Wolk, L. McCluskey, L. Elman, V. Kostanjevecki, M. Vandijck, J. McBride, J. Q. Trojanowski, K. Blennow, Elevated CSF GAP-43 is Alzheimer's disease specific and associated with tau and amyloid pathology, *Alzheimers Dement.* 15 (1) (2019) 55–64.
- [23] M. Suarez-Calvet, E. Morenas-Rodriguez, G. Kleinberger, K. Schlepckow, M. A. Araque Caballero, N. Franzmeier, A. Capell, K. Fellerer, B. Nuscher, E. Eren, J. Levin, Y. Deming, L. Piccio, C.M. Karch, C. Cruchaga, L.M. Shaw, J. Q. Trojanowski, M. Weiner, M. Ewers, C. Haass, I. Alzheimer's Disease Neuroimaging, Early increase of CSF sTREM2 in Alzheimer's disease is associated with tau related-neurodegeneration but not with amyloid-beta pathology, *Mol. Neurodegener.* 14 (1) (2019) 1.
- [24] V. Ovod, K.N. Ramsey, K.G. Mawuenyega, J.G. Bollinger, T. Hicks, T. Schneider, M. Sullivan, K. Paumier, D.M. Holtzman, J.C. Morris, T. Benzinger, A.M. Fagan, B. W. Patterson, R.J. Bateman, Amyloid beta concentrations and stable isotope labeling kinetics of human plasma specific to central nervous system amyloidosis, *Alzheimers Dement.* 13 (8) (2017) 841–849.
- [25] T.K. Karikari, T.A. Pascoal, N.J. Ashton, S. Janelidze, A.L. Benedet, J.L. Rodriguez, M. Chamoun, M. Savard, M.S. Kang, J. Therriault, M. Scholl, G. Massarweh, J. P. Soucy, K. Hoglund, G. Brinkmalm, N. Mattsson, S. Palmqvist, S. Gauthier, E. Stomrud, H. Zetterberg, O. Hansson, P. Rosa-Neto, K. Blennow, Blood phosphorylated tau 181 as a biomarker for Alzheimer's disease: a diagnostic performance and prediction modelling study using data from four prospective cohorts, *Lancet Neurol.* 19 (5) (2020) 422–433.
- [26] N. Mattsson, U. Andreasson, H. Zetterberg, K. Blennow, I., Alzheimer's disease neuroimaging, Association of Plasma Neurofilament Light with neurodegeneration in patients with Alzheimer disease, *JAMA Neurol.* 74 (5) (2017) 557–566.
- [27] C.R. Jack Jr., M.A. Bernstein, N.C. Fox, P. Thompson, G. Alexander, D. Harvey, B. Borowski, P.J. Britson, J.L. Whitwell, C. Ward, A.M. Dale, J.P. Felmlee, J. L. Gunter, D.L. Hill, R. Killiany, N. Schuff, S. Fox-Bosetti, C. Lin, C. Studholme, C. S. DeCarli, G. Krueger, H.A. Ward, G.J. Metzger, K.T. Scott, R. Mallozzi, D. Blezek, J. Levy, J.P. Debbins, A.S. Fleisher, M. Albert, R. Green, G. Bartzokis, G. Glover, J. Mugler, M.W. Weiner, The Alzheimer's disease neuroimaging initiative (ADNI): MRI methods, *J. Magn. Reson. Imaging* 27 (4) (2008) 685–691.
- [28] S.M. Landau, D. Harvey, C.M. Madison, R.A. Koeppe, E.M. Reiman, N.L. Foster, M. W. Weiner, W.J. Jagust, I., Alzheimer's disease neuroimaging, associations between cognitive, functional, and FDG-PET measures of decline in AD and MCI, *Neurobiol. Aging* 32 (7) (2011) 1207–1218.
- [29] T.G. Gorgels, M. Van Lookeren Campagne, A.B. Oestreicher, A.A. Gribnau, W. H. Gispen, B-50/GAP43 is localized at the cytoplasmic side of the plasma membrane in developing and adult rat pyramidal tract, *J. Neurosci.* 9 (11) (1989) 3861–3869.
- [30] M. Tible, A. Sandelius, K. Hoglund, A. Brinkmalm, E. Cognat, J. Dumurgier, H. Zetterberg, J. Hugon, C. Paquet, K. Blennow, Dissection of synaptic pathways through the CSF biomarkers for predicting Alzheimer disease, *Neurology* 95 (8) (2020) e953–e961.
- [31] Q. Qiang, L. Skudder-Hill, T. Toyota, W. Wei, H. Adachi, CSF GAP-43 as a biomarker of synaptic dysfunction is associated with tau pathology in Alzheimer's disease, *Sci. Rep.* 12 (1) (2022) 17392.
- [32] G. Kleinberger, Y. Yamanishi, M. Suarez-Calvet, E. Czirr, E. Lohmann, E. Cuyvers, H. Struyfs, N. Pettkus, A. Wenninger-Weinzierl, F. Mazaheri, S. Tahirovic, A. Lleo, D. Alcolea, J. Fortea, M. Willem, S. Lammich, J.L. Molinuevo, R. Sanchez-Valle, A. Antonell, A. Ramirez, M.T. Heneka, K. Sleegers, J. van der Zee, J.J. Martin, S. Engelborghs, A. Demirtas-Tatlidede, H. Zetterberg, C. Van Broeckhoven, H. Gurvit, T. Wyss-Coray, J. Hardy, M. Colonna, C. Haass, TREM2 mutations implicated in neurodegeneration impair cell surface transport and phagocytosis, *Sci. Transl. Med.* 6 (243) (2014) 243ra86.
- [33] K. Schlepckow, G. Kleinberger, A. Fukumori, R. Feederle, S.F. Lichtenthaler, H. Steiner, C. Haass, An Alzheimer-associated TREM2 variant occurs at the ADAM cleavage site and affects shedding and phagocytic function, *EMBO Mol. Med.* 9 (10) (2017) 1356–1365.
- [34] M. Suarez-Calvet, G. Kleinberger, M.A. Araque Caballero, M. Brendel, A. Rominger, D. Alcolea, J. Fortea, A. Lleo, R. Blesa, J.D. Gisbert, R. Sanchez-Valle, A. Antonell, L. Rami, J.L. Molinuevo, F. Brosseron, A. Traschütz, M.T. Heneka, H. Struyfs, S. Engelborghs, K. Sleegers, C. Van Broeckhoven, H. Zetterberg, B. Nellgard, K. Blennow, A. Crispin, M. Ewers, C. Haass, sTREM2 cerebrospinal fluid levels are a potential biomarker for microglia activity in early-stage Alzheimer's disease and associate with neuronal injury markers, *EMBO Mol. Med.* 8 (5) (2016) 466–476.
- [35] N. Mattsson, M. Scholl, O. Strandberg, R. Smith, S. Palmqvist, P.S. Insel, D. Hagerstrom, T. Ohlsson, H. Zetterberg, J. Jogi, K. Blennow, O. Hansson, (18)F-AV-1451 and CSF T-tau and P-tau as biomarkers in Alzheimer's disease, *EMBO Mol. Med.* 9 (9) (2017) 1212–1223.
- [36] S. Janelidze, E. Stomrud, R. Smith, S. Palmqvist, N. Mattsson, D.C. Airey, N. K. Proctor, X. Chai, S. Shcherbinin, J.R. Sims, G. Triana-Baltzer, C. Theunis, R. Slemmon, M. Mercken, H. Kolb, J.L. Dage, O. Hansson, Cerebrospinal fluid p-tau217 performs better than p-tau181 as a biomarker of Alzheimer's disease, *Nat. Commun.* 11 (1) (2020) 1683.
- [37] A. Leuzy, S. Janelidze, N. Mattsson-Carligen, S. Palmqvist, D. Jacobs, C. Cicognola, E. Stomrud, E. Vanmechelen, J.L. Dage, O. Hansson, Comparing the clinical utility and diagnostic performance of CSF P-Tau181, P-Tau217, and P-Tau231 assays, *Neurology* 97 (17) (2021) e1681–e1694.